

# Mass-Spectrometric Studies of the Interactions of Selected Metalloantibiotics and Drugs with Deprotonated Hexadeoxynucleotide GCATGC

Janna Anichina and Diethard K. Bohme\*

Department of Chemistry and Centre for Research in Mass Spectrometry, York University, 4700 Keele Street, Toronto, Ontario, Canada M3J 1P3

Received: August 6, 2008; Revised Manuscript Received: October 31, 2008

ESI tandem mass spectrometry is employed in a detailed study of the interactions of a hexameric duplex d(5'GCATGC) with three types of ligated first-row transition metal dications  $M^{2+}$ : metallated bleomycins, singly, doubly, and triply ligated metallophenanthrolines and  $[M(\text{triethylenetetramine})]^{2+}$ . The singly, doubly, and triply metallated species were found to dissociate by noncovalent separation into two strands with metal ions attached either to one or to both. Relative gas-phase stabilities of the double-stranded oligodeoxynucleotide (ODN)– $M^{2+}$  complexes were found to follow the order  $\text{Mn(II)} > \text{Fe(II)} > \text{Co(II)} > \text{Ni(II)} > \text{Zn(II)} > \text{Cu(II)}$ . Overall, the presence of metal dications is found to increase the gas-phase stability of the duplex against noncovalent dissociation with the exception of one and three copper dications. An analysis of the dissociation pathways and relative gas-phase stabilities of the species that were investigated provided a basis for the assessment of the possible binding modes between duplex oligonucleotides and metallocomplexes.

## Introduction

Understanding how to target different DNA sites with chemical specificity is extremely important from the point of view of designing novel chemotherapeutics as well as expanding our knowledge of efficient probes of DNA structure and sensitive diagnostic agents.<sup>1</sup> Transition metal ions have been of great interest in controlling and developing the molecular architecture of nucleic acids and their derivatives since the 1950s. They are well-known to be capable of interacting with donor atoms of both the phosphodiester backbone and nucleobases of DNA. Major and minor grooves of DNA coordinate metal cations in a sequence-specific manner that arises from the overall electrostatic character of their grooves and specific positions of electronegative groups in these grooves.<sup>2</sup> Coordinated with small molecules and drugs, transition metal ions can bind and react at specific sequences of DNA.<sup>3</sup> For example, binding of Mg–quinobenzoxazine, Mg–aureolic acid, cisplatin, and Fe–bleomycin with nucleic acids impairs their function and/or initiates their cleavage.<sup>4</sup>

An accurate assessment of the binding mode (modes) of a metallocomplex with DNA requires a demonstration of changes in the physicochemical properties of the latter occurring upon binding. For instance, intercalation within DNA is accompanied by its unwinding, lengthening, and stiffening, as well as electronic interactions of the intercalator with the DNA. Experiments that reveal such changes include those that demonstrate changes in the solution viscosity, sedimentation coefficient or electrophoretic mobility of the bulk DNA and/or a shift to a longer wavelength of the transition of the intercalated species.<sup>5–7</sup> Luminescence polarization experiments that establish the time over which an intercalator is rigidly bound within the helix would also contribute to the confirmation of the nature of intercalative binding. The advent of electrospray ionization (ESI)<sup>8,9</sup> has spawned tremendous advances in the structural characterization of biomolecules such as DNA and oligodeoxynucleotides (ODNs), their metallated adducts, and noncovalent complexes with proteins and drugs.<sup>10–26</sup> Collision induced dissociation (CID) has proven to be a powerful tool in providing

important information regarding the sequence of ODNs and probable sites for the binding of metal ions.<sup>27–30</sup> Considerable attention has been focused on the capabilities of ESI-MS/MS in distinguishing binding modes of small ligands with duplexes and triplexes of DNA on the basis of their CID pathways and energetics.<sup>31–35</sup> However, all these studies have been dedicated to direct ligand–ODN interactions. In our laboratory we have concentrated on exploring the capabilities of ESI-MS/MS technique in the investigations of the interaction of DNA models with small molecules and drugs mediated by the first row transition metal dications, and this will be the focus of this publication. We have chosen a relatively short, self-complementary hexadeoxynucleotide d(5'GCATGC) as the nucleic acid of interest because of its high GC content, its previous use by bioinorganic chemists in structural studies,<sup>36</sup> and the mass range of the mass spectrometer (up to  $m/z$  1800). Even though a hexameric duplex is not long enough to form a helical turn, which requires at least 10 base pairs, it does contain important elements of a helix such as backbone torsions, sugar conformations, and glycosidic bonds for pyrimidines.<sup>36</sup> Also, d(5'GCATGC) is a self-complementary Watson–Crick type sequence that reduces the number of species that are formed in solution.

The ligands that were selected (bleomycin A<sub>2</sub>, 1,10-phenanthroline, and triethylenetetraamine) are known to form stable complexes with the first row transition metal ions as well as ternary adducts with DNA in the presence of these metal ions. Metallocomplexes of bleomycin are currently utilized in treatment of certain types of tumors.<sup>4</sup> 1,10-Phenanthroline is commonly used in the synthesis of efficient metallointercalators and DNA oxidizing agents.<sup>1</sup> Triethylenetetraamine, a member of the polyamine family known to interact electrostatically with the phosphodiester backbone of DNA, is of fundamental interest. Also, it is used for the treatment of Wilson's disease, an autosomal recessive disorder characterized by copper accumulation in various organs, such as the liver, kidney, and brain.<sup>37</sup>

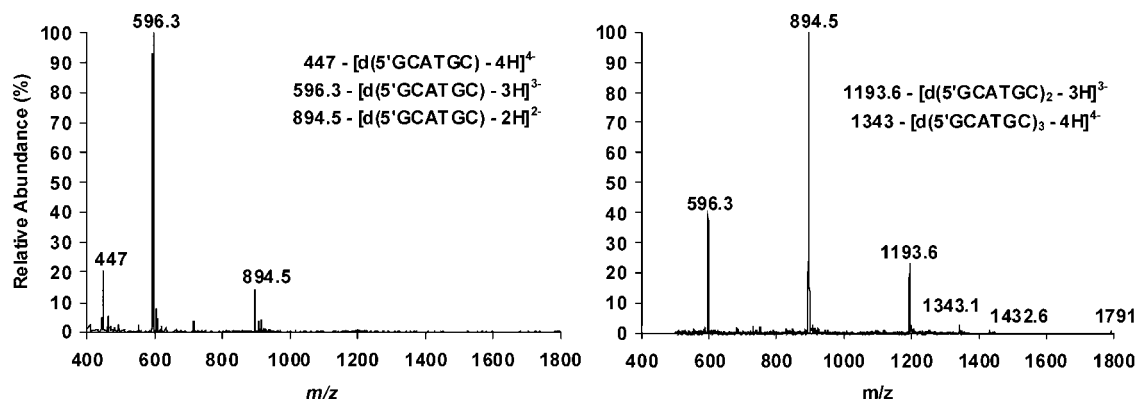


Figure 1. ESI mass spectra of 20  $\mu$ M solutions of d(5'GCATGC) in 20:80 methanol:water (left) and annealed in the  $\text{NH}_4\text{CH}_3\text{CO}_2$  (right).

## Experimental Procedures

Electrospray data were acquired in the negative ion mode using an API 2000 (MDS-SCIEX, Concord, ON, Canada) triple quadrupole ( $Q_1Q_2Q_3$ ) mass spectrometer equipped with a "Turbo Ion Spray" ion source. Experiments were performed at an ion spray voltage of  $-5500$  V, a ring-electrode potential of  $-300$  V (used for ion beam confinement), and a range of potential differences between the orifice and the skimmer.  $\text{N}_2$  was used as a curtain gas at a setting of 10 psi and air was used as a nebulizer at a flow rate of  $8 \text{ L min}^{-1}$ . Samples were directly infused into the electrospray source at a flow rate of  $3 \mu\text{L min}^{-1}$ .

MS/MS was performed in the product ion and multiple reaction monitoring (MRM) modes with  $\text{N}_2$  as collision gas at a pressure estimated to be about 3 mTorr (viz. multicollision conditions). The collision offset voltage (the potential difference between the quadrupole entrance lens ( $q_0$ ) and the collision cell quadrupole ( $q_2$ )), which nominally gives the laboratory frame collision voltage, was adjusted between  $-1$  and  $-130$  V at 1 V intervals. Space charge and contact potentials, field penetration, and field distortion all can influence the actual collision voltage but were not taken into account. Product ion spectra were obtained by scanning  $Q_3$  over the range  $m/z = 10$ – $1800$ . The interquadrupole lens potentials and the float potential of the resolving quadrupole  $Q_3$  were linked to the  $q_2$  potential to maintain proper transmission through  $Q_3$ .

The relative gas-phase stability of a particular ion in this study was evaluated utilizing so-called tangent voltage value (TV), determined by extrapolating the steepest slope of the parent ion breakdown curve to the collision voltage axis.<sup>38</sup> The precision of the TVs is taken to be one standard deviation from the mean TV value obtained in several (four or more) repeated experiments. In each experiment, Gaussian smoothing was applied twice to the ion signals measured at each collision voltage, each accumulated for a dwell time of 500 ms, in order to remove local variations caused by noise. Double smoothing was applied to improve the fit of the linear portion of the disappearance curve of the parent ion used in the determination of the TV value. Although a slight bias ( $<5\%$ ) is introduced in this way to the raw data, the bias is systematic and does not influence the relative order of TV values. The TVs were not measured as a function of pressure.

Ligated Mn (II), Co(II), Ni(II), Cu(II), and Zn (II) were generated from their nitrate hydrates (Aldrich,  $\text{pa} \geq 99.99\%$ ) while iron(II) sulfate heptahydrate (Aldrich,  $\text{pa} \geq 98\%$ ) was used as the source of Fe(II) ions; triethylenetetramine (trien) hydrochloride, 1,10-phenanthroline (phen), and blenoxane (BLM) were purchased from Aldrich  $\text{pa} \geq 98\%$  and used without further purification. HPLC grade methanol and Millipore (18.2

m $\Omega$ ) water were used to prepare the solvent mixture. An oligodeoxynucleotide (ODN) with a d(5'GCATGC) sequence, purchased from ACGT Corporation (Toronto), was desalted and cartridge purified. In order to form double-stranded species, the ODN was annealed in 100 mM solution of ammonium acetate buffer by heating to  $90^\circ\text{C}$  for 15 min and slow cooling down to room temperature over a 3-h period. Stock solutions were diluted in 20:80 methanol:water mixture to yield a 20  $\mu$ M solution. Trien, phen, and BLM were dissolved in 20:80 methanol:water mixture at a concentration of 10  $\mu$ M and the appropriate metal salt was added to 5-fold molar excess. The 100 mM solution of ammonium acetate also was prepared in a 20:80 methanol:water mixture so that the ratio of the solvents did not change in the final electrosprayed solutions in which the concentration of ammonium acetate was about 50 mM.

## Results and Discussion

**Formation and Dissociation of the Bare Deprotonated Duplex.** The negative ion mass spectrum of the deprotonated duplex of the ODN chosen for study is shown in Figure 1. The mass spectrum on the left side of the figure reflects the composition of a 20  $\mu$ M solution of the ODN in the absence of ammonium acetate buffer, while that on the right side demonstrates the composition of the solution after annealing. The latter procedure insures nucleic acid hybridization, the process of combining complementary, single-stranded nucleic acids into a single molecule.<sup>39</sup> Nucleotides will bind to their complement under normal conditions, so two perfectly complementary strands will bind to each other readily. The experimental annealing procedure involves the following steps: (1) the double-stranded DNA or oligodeoxynucleotide is heated in solution, usually buffered for pH; (2) due to external conditions, the hydrogen-bonded base pairing becomes thermodynamically unfavorable and the complementary strands separate; (3) one strand of denatured DNA is then mixed with another set of denatured DNA and the combined sets are then cooled slowly to allow the DNA to reanneal and form a new "hybridized" DNA molecule.<sup>39</sup> Figure 1 illustrates a sharp increase in the yield of the double-stranded species upon annealing.

We focused our studies on the double-stranded species with an odd number of charges ( $3-$ ) to avoid the ambiguity in the peak assignments that arises for double-stranded ODN ions carrying an even number of charges that have the same mass-to-charge ratio as single-stranded ones with half the charge.

Figure 3 shows that the dissociation of the double-stranded trianion of the triply deprotonated hexamer results in the separation into two strands, singly and doubly charged, respectively.

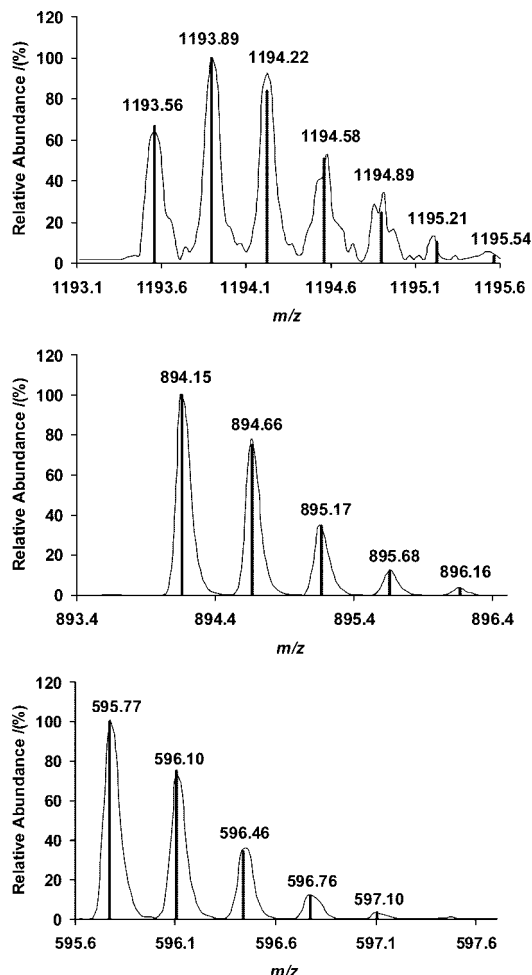


**Figure 2.** Enhanced resolution scans acquired for  $[d(5'GCATGC)_2-3H]^{3-}$  (1193.8),  $[d(5'GCATGC)-3H]^{3-}$  (596.7), and  $[d(5'GCATGC)-2H]^{2-}$  (894.2) utilizing a Q trap 2000 instrument along with the theoretical isotopic distribution (shown as solid lines).

The TV value of the dissociation of the self-complementary trianion of  $d(5'GCATGC)$  was measured to be  $-30.7 \pm 0.2$  V, and the dissociation was observed to result only in the separation into two strands, singly and doubly charged, respectively. Others have reported similar dissociations of other deprotonated self-complementary double-stranded ODNs in different charge states and various lengths using a variety of mass spectrometers.<sup>17,18,40</sup> Onset energies (TV values) for strand separation were not reported previously. A further dissociation of the doubly charged single strand product into singly charged sequence ions is seen in Figure 3 at higher collision voltages (the complementary anion, not labeled in Figure 3, is observed at lower intensities and dissociates further). Separate experiments in which the single stranded dianion is selected and subjected to CID show the same dissociation. Again, others appear to have observed similar dissociations.<sup>17,18,40</sup>

**Metallocomplexation of the Single- and Double-Stranded ODNs: CID Pathways of the Multiply Metallated Species.** Addition of different excesses of the salts of the first row transition metal dications to the annealed solution of  $d(5'GCATGC)$  results in the formation of multiply metallated species. Addition of up to two metal dications was observed for the single-stranded ions in the charge state  $2-$  and up to four for the double-stranded ODN in charge state  $3-$ . A shift in the distribution of the intensities of the species with different numbers of the attached metal dications was observed upon an increase in the

concentration of the corresponding metal salt: the larger the excess of the metal salt, the higher were the yields of multiply metallated species (Figure 4). The latter observation suggests that the yields of the ions in the ESI spectra of the metal–ODN systems reflect their solution distribution, although denaturation in solution caused by excessive concentrations of metal ions and nonspecific addition in the electrospray process cannot be excluded.

The net charges on the observed ions in Figure 4 in the presence of the metal dications provide a measure of the number of deprotonations of the ODN. Since the phosphate groups are fully deprotonated at the pH (ca. 6.5) of the solutions that were used, the (positive) metal dications can be expected to preferentially bind to these (negative) sites within the backbone rather than to the nucleobases that are involved in Watson–Crick hydrogen bonding. The overall number of the phosphates in a double-stranded hexadeoxynucleotide is 10. In order to achieve a charge state of  $3-$  upon addition of a metal dication, 5 protons should dissociate from the molecule, the addition of 2 dications requires the loss of 7 protons, 3 dications will require loss of 9 protons, and 4 will require 11 protons to be lost. So, in the case of a quadruply metallated trianion of the hexameric duplex, in addition to a complete deprotonation of all the phosphate groups that are present, an extra proton should be lost to achieve the observed charge state. The latter may lead to a disruption in pairing of the nucleobases, possibly by duplex “unzipping” and, eventually, to the dissociation into two separate strands.<sup>39</sup> We assume here that first row transition metal dications prefer to bind with deprotonated phosphates and nucleobases rather than with deprotonated hydroxyl groups of sugars as has been demonstrated in many other studies.<sup>41</sup> Furthermore, it is well-known that metal cations that bind primarily to the phosphate backbone will stabilize the double-stranded conformation over and above the hydrogen that is still expected to be present, whereas those that bind to the bases will tend to denature the duplex.<sup>41</sup> Figure 4 (right side spectrum) illustrates the drop in the relative abundance of the metallated species with 1–4 attached metal dications. Higher metallations were not observed under the chosen conditions of concentration. This may be the consequence of partial unzipping of the duplex at the higher concentrations of the metal salts due to the disruption of hydrogen bonding induced by interactions of the additional metal ions with the nucleobases. Complete unzipping is unlikely since the double-stranded trianion is still present in the ESI spectrum of the ODN/metal ion solution.

In order to gain insight into the gas-phase structure of the metal complexes of the single- and double-stranded ODN, we performed MS/MS of the singly, doubly, and triply metallated species. Dissociation pathways of both metallated and nonmetallated single strand containing ions were similar in that they were charge-directed. Higher charge states ( $3-$ ) were found to dissociate by charge separation associated with the loss of a deprotonated base, while lower charge states ( $2-$ ) tended to shed a neutral base. Overall, dianions of the single-stranded ODN containing one and two dications of the first row transition metals exhibited greater stability toward CID compared to the bare single strands. The latter observation is consistent with the earlier studies by Wang et al.<sup>42</sup> with  $Na^+$ ,  $K^+$ ,  $Li^+$ ,  $Cs^+$ ,  $Mg^{2+}$ , and  $Ca^{2+}$ .

MS/MS experiments performed with the double-stranded species indicate that all metallated duplexes dissociate noncovalently forming two single strands with metal ions still attached to one of them or to both depending on the extent of metallation. Reactions 1–5 summarize the dissociation pathways for the

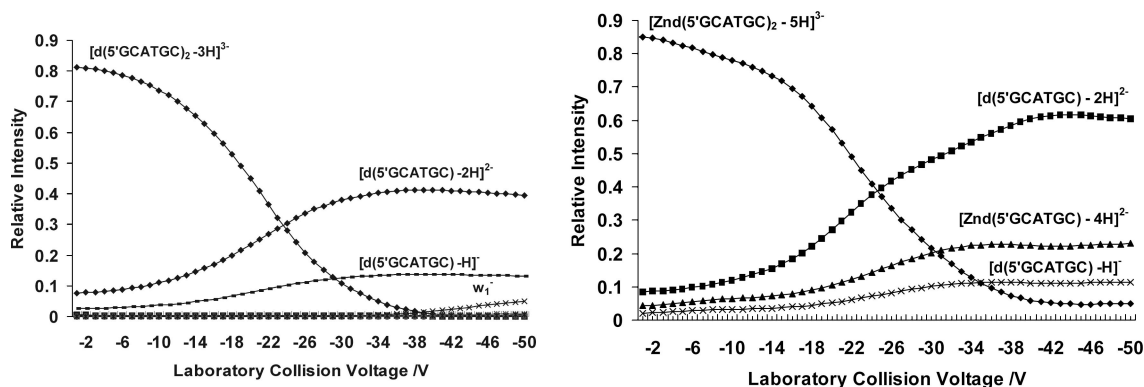


Figure 3. CID profiles for the dissociation  $[d(5'GCATGC)_2-3H]^{3-}$  (left) and  $[Zn d(5'GCATGC)_2-5H]^{3-}$  (right).

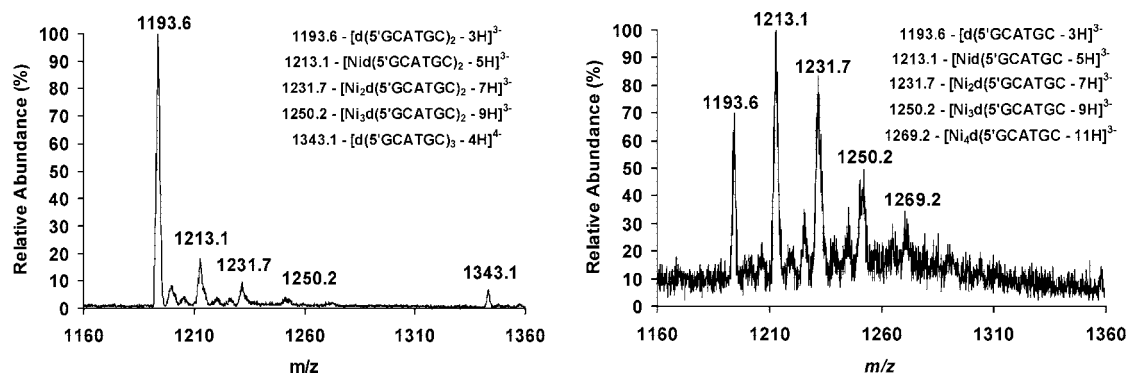


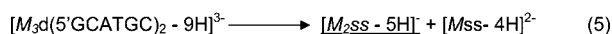
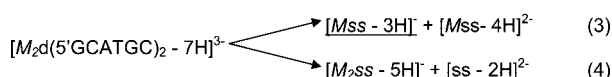
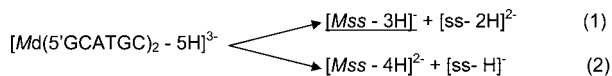
Figure 4. ESI spectra of the solutions containing previously annealed  $d(5'GCATGC)$  ( $20 \mu M$ ) with 10-fold excess (right) and 5-fold (left) of nickel nitrate in 20:80 methanol/water.

TABLE 1: Tangent Voltages (in volts) for Singly, Doubly, and Triply Metallated Duplexes of the First Row Transition Metal Dications<sup>a</sup>

$M^{2+}$	$[Md(5'GCATGC)_2-5H]^{3-}$	$[M_2d(5'GCATGC)_2-7H]^{3-}$	$[M_3d(5'GCATGC)_2-9H]^{3-}$
$Mn^{2+}$	$-46.7 \pm 0.3$ (1.07)	$-44.0 \pm 0.4$ (0.99)	$-43.2 \pm 0.4$ (0.96)
$Fe^{2+}$	$-43.7 \pm 0.3$ (1.00)	$-41.6 \pm 0.7$ (0.94)	$-39.2 \pm 0.4$ (0.87)
$Co^{2+}$	$-40.0 \pm 0.4$ (0.92)	$-34.7 \pm 0.5$ (0.78)	$-36.5 \pm 0.4$ (0.81)
$Ni^{2+}$	$-38.7 \pm 0.4$ (0.87)	$-36.1 \pm 0.4$ (0.81)	$-36.1 \pm 0.4$ (0.80)
$Cu^{2+}$	$-29.4 \pm 0.3$ (0.68)	$-34.1 \pm 0.4$ (0.77)	$-28.6 \pm 0.3$ (0.63)
$Zn^{2+}$	$-35.6 \pm 0.4$ (0.81)	$-33.8 \pm 0.4$ (0.76)	$-33.1 \pm 0.3$ (0.73)

<sup>a</sup> The corresponding apparent center of mass (CM) energies (in electronvolts) are given in parentheses. The apparent center of mass energies were calculated according to  $E_{CM}^a = zTVm_{N_2}(m_{N_2} + m_{ion})^{-1}$  where  $z$  represents the charge of the corresponding parent ion.

observed complexes of the first row transition metal dications with deprotonated  $d(5'GCATGC)_2$ . The singly charged ions that are underlined were not observed due to the limitations in the available range in  $m/z$ . The dissociation of singly metallated



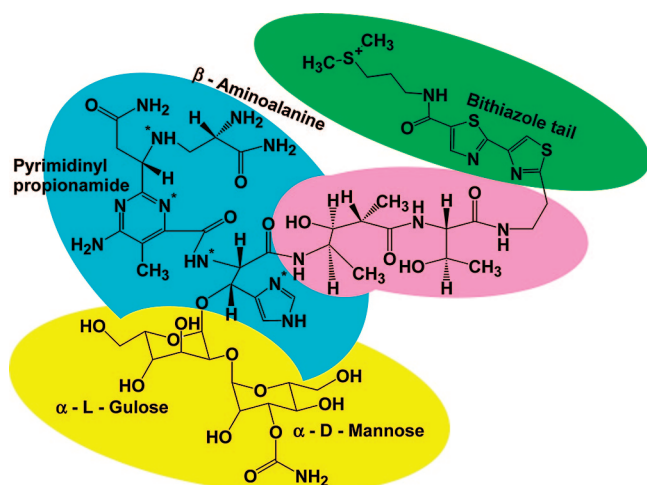
species was found to proceed via separation into two strands by two competing channels 1 and 2. Pathway 1 dominates with  $M = Mn, Fe, Co$ , and  $Ni$  while both pathways 1 and 2 occur with  $M = Cu$  and  $Zn$  and in relatively equal amounts (Figure 3). Doubly metallated ODNs also fragment via two channels with reaction 3 being predominant for all the metal dications.

$[d(5'GCATGC-3H)]^{3-}$  species with three metal dications attached exhibited only one fragmentation pathway, reaction 5. MS/MS experiments could not be performed with quadruply metallated trianions due to the very low yields of these ions. The relative gas-phase stabilities of the different trianionic metallocomplexes of the double-stranded ODN are compared in Table 1.

The tangent voltage value for the bare trianion of the duplex was found to be  $-30.7 \pm 0.2$  V (0.71 eV in the apparent center of mass frame). Table 1 indicates that metallocomplexation increases the gas-phase stability of the double-stranded ODN with the exception of singly and triply metallated copper adducts. The presence of metal ions in the structure of the double-stranded ODN is expected to relieve Coulombic strain by interacting with its polyanionic phosphodiester backbone and so increase gas-phase stability. The TV values that were observed for the metallated ODN also indicate that the interaction of the metal ion(s) and the nucleic acid takes place with the deprotonated phosphate groups of both strands, otherwise we could expect the stabilities of the metallated species against CID to be similar to that of the bare  $(d(5'GCATGC)_2-3H)^{3-}$ .

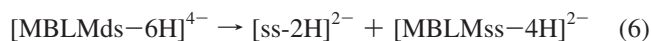


## SCHEME 1



**M<sup>2+</sup>–Bleomycin A<sub>2</sub>–d(5'GCATGC).** The bleomycins (BLMs) are natural products clinically employed in combination chemotherapy in the treatment of lymphomas, cervical cancers, and squamous cell carcinomas of the head and neck.<sup>4,43,44</sup> The mode of cytotoxicity of BLMs is believed to be related to their ability to cleave nucleic acids in the presence of the metal cofactor(s), O<sub>2</sub>, and a reductant.<sup>43</sup> The structure of bleomycin A<sub>2</sub><sup>+</sup> is presented in Scheme 1. There are four distinct domains (colored) in the structure of the species: (i) the metal-binding domain (blue) responsible for the coordination with a metal cation (four N atoms with asterisks are believed to coordinate a central ion in the equatorial plane<sup>43</sup> while the amino group belonging to the β-aminoalanine moiety provides one axial ligand leaving the sixth coordination site available for a solvent molecule (or some other ligand); (ii) the disaccharide domain (yellow); (iii) the linker-peptide region (pink); and (iv) the DNA-binding domain (green). The bithiazole tail is responsible for multiple modes of DNA binding, including probable partial intercalation and binding within the minor groove, that were suggested in some in vitro experiments.<sup>43,44</sup> Formation of the ternary adducts of metallated bleomycin with the single- or double-stranded ODN was observed in our experiments upon the addition of an equimolar (with respect to the concentration of single-stranded hexanucleotide) amount of Blenoxane (a mixture of several forms of bleomycin with 70% content of the A<sub>2</sub> form) to the solution of a metal ion mixed with the annealed ODN.

In the elucidation of peaks, MS/MS experiments were performed with the most intense multiply charged negative ions that dissociate into products with *m/z* within the available mass range, viz. [MBLMd(5'GCATGC)–5H]<sup>3–</sup> and [MBLMd(5'GCATGC)<sub>2</sub>–6H]<sup>4–</sup> (M = Mn, Co, Ni, Cu, and Zn; BLM = bleomycin A<sub>2</sub><sup>+</sup>–H<sup>+</sup>). Upon coordination of the metal cation within the metal-binding domain of bleomycin A<sub>2</sub><sup>+</sup>, a proton leaves the amido group and is replaced by the metal cation. The dissociation pathway for the latter anion, reaction 6 with ds and ss being double- and single-stranded ODN, respectively, was found to be identical for Mn-, Co-, Ni-, and Cu-containing complexes.



An example of a CID profile that illustrates the occurrence of reaction 6 is presented by Figure 5.

The Zn(II)-containing adduct was observed to be special in that it dissociated via two channels, one similar to the rest of the metallocomplexes, reaction 6, and the other according to reaction 7.



The special behavior of the Zn-containing adduct might be explained in terms of softness/hardness of the metal ions that were chosen for study. The first-row transition metal dications cannot be classified either as soft or hard but rather can be considered to exhibit borderline properties.<sup>41</sup> However, Zn<sup>2+</sup> (d<sup>10</sup> configuration) is the hardest among the first-row transition metal dications and much closer in properties to alkali-earth dications. On the other hand, nucleic acids offer a plethora of binding sites for metal ions, such as phosphate groups, nucleobases, and deoxyriboses. As was demonstrated previously,<sup>41</sup> hard metal dications such as Mg<sup>2+</sup> and Ca<sup>2+</sup> prefer phosphate groups. The CID pathway of Zn-containing adduct that was observed to be minor suggests that the affinity of the zinc dication for the phosphate groups of the ODN is comparable to that for BLM in the gas phase. The CID profiles of the corresponding tetra-anion of d(5'GCATGC)<sub>2</sub> are presented in Figure 5.

Tangent voltages (in volts) and corresponding apparent center of mass energies (in electronvolts) given in parenthesis of metallobleomycin complexes with double-stranded d(5'GCATGC)<sub>2</sub> for Mn<sup>2+</sup>, Co<sup>2+</sup>, Ni<sup>2+</sup>, Cu<sup>2+</sup>, and Zn<sup>2+</sup> were found to be  $-35.4 \pm 0.7$  (0.78),  $-34.7 \pm 0.5$  (0.76),  $-32.4 \pm 0.6$  (0.72),  $-31.4 \pm 0.8$  (0.69), and  $-31.8 \pm 0.6$  (0.70), respectively. Since  $E_{\text{CM}}^{\text{app}}$  for the bare double-stranded ODN was found to be 0.71 eV, these values indicate that the attachment of the metallobleomycins to the double-stranded ODN does not significantly change the amount of energy required to separate two strands via breakage of the hydrogen bonds between Watson–Crick base pairs. This result suggests that metal ions are not directly involved in the interaction with the oligodeoxynucleotide but rather a different part of the metallated bleomycin is responsible for the binding with the ODN. Solution studies<sup>43,44</sup> have shown that this binding indeed occurs via the bithiazole tail of BLM called the DNA-binding domain of the ligand. So it is likely that nothing changes upon transfer from the solution to the gas phase. However, the mode of the binding is still under discussion.<sup>43,44</sup> Our gas-phase results suggest that the DNA-binding domain of BLM forms hydrogen bonds with only one of the strands in the duplex probably via its secondary amino group (a proton donor) and/or the nitrogen atoms of the bithiazole rings (proton acceptors), rather than intercalating the bithiazole rings between the base pairs of the duplex. Therefore, the dissociation pathways of the [MBLMd(5'GCATGC)<sub>2</sub>–6H]<sup>4–</sup> with M = Mn, Co, Ni, Cu, and Zn, along with their gas-phase stabilities (TV values), provide evidence for the groove binding of MBLM<sup>2+</sup> with d(5'GCATGC)<sub>2</sub>. A comparable observation has been reported by Rosu et al.<sup>15,34</sup> who investigated complexation of duplex DNA with minor groove binders (Hoechst 33258 and 33342, netropsin, and DAPI) and intercalators (daunomycin, doxorubicin, actinomycin D, ethidium, cryptolepine, neocryptolepine, *m*-Amsacrine, proflavine, ellipticine, and mitoxantrone) by ESI-MS and ESI-MS/MS in the negative ion and positive ion modes. Dissociation of the duplexes with the selected groove binders was found in the negative ion mode to proceed via separation into two strands with the ligand attached to one of them. Some of the

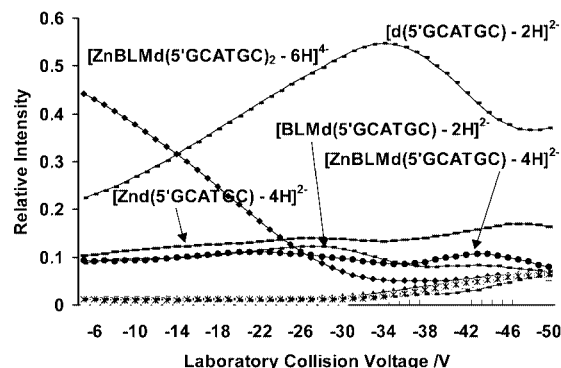
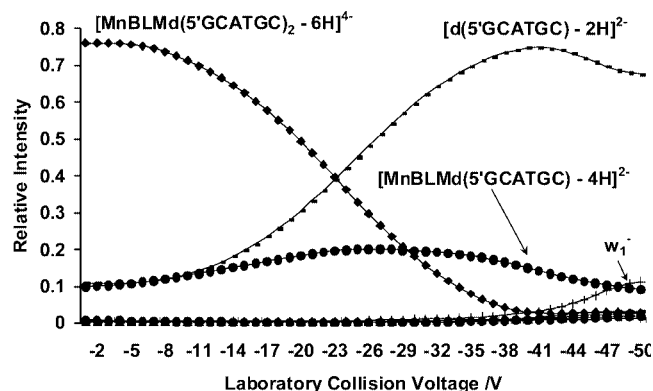
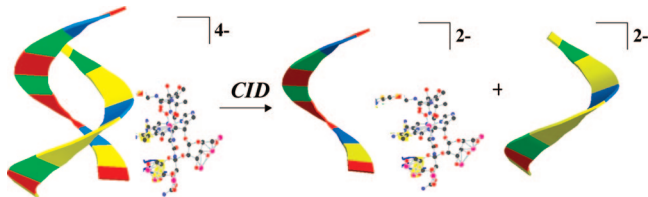
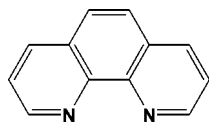


Figure 5. CID profiles for the dissociation of  $[\text{ZnBLMd}(5'\text{GCATGC})_2 - 6\text{H}]^{2-}$  (right) and  $[\text{MnBLMd}(5'\text{GCATGC})_2 - 6\text{H}]^{2-}$  (left).

#### SCHEME 2



#### SCHEME 3



intercalators were observed to separate from the duplexes as neutrals.<sup>34</sup> Therefore, if the bithiazoles in the bleomycin were intercalated into  $\text{d}(5'\text{GCATGC})_2$  in our experiments, we should expect a different fragmentation pattern (loss of a neutral bleomycin for instance) and a disruption in the stacking of the bases and so a change in the gas-phase stabilities ( $E_{\text{M}}^{\text{ap}}$ ) of the ternary adducts compared to the stability of the bare double-stranded ODN. On the other hand, groove binders are known to stabilize the helical structure of DNA due to their crescentlike shapes that are well adapted for interactions with the pitch and curvature of the minor groove of helical DNA.<sup>45,46</sup> Even though a hexameric duplex  $\text{d}(5'\text{GCATGC})_2$  is too short to form a helix that requires at least 10 bases in the sequence, the DNA-binding domain of bleomycin can form hydrogen bonds with the phosphodiester backbone of one of the strands in the duplex without interfering with the Watson–Crick base pairing. The CID of such a construct may be visualized in Scheme 2.

**$\text{M}^{2+}$ –1,10-Phenanthroline– $\text{d}(5'\text{GCATGC})_2$  System.** 1,10-Phenanthroline (phen) (see Scheme 3) is a bidentate ligand that coordinates with first-row transition metal dications via the lone pairs of its two nitrogens.<sup>38</sup>

Fluorescence spectroscopy and ultraviolet spectroscopy techniques combined with cyclic voltammetry have been used by others to study the interaction between  $[\text{Co}(\text{phen})_2(\text{Cl})(\text{H}_2\text{O})]\text{Cl} \cdot \text{H}_2\text{O}$  and salmon sperm DNA as a model DNA. Results show that  $[\text{Co}(\text{phen})_2(\text{Cl})(\text{H}_2\text{O})]^+$  binds to double-strand DNA by intercalation.<sup>47</sup> The most extensively studied metal complex of phenanthroline is the doubly charged ruthenium trisphenanthroline which is of interest because of its fluorescent nature which is useful in the detection of its binding to DNA.<sup>48</sup> This complex also serves as the platform for the creation of fluorescent metal intercalators that bond to oligodeoxynucleotides with high specificity.<sup>1</sup> The binding mode of ruthenium

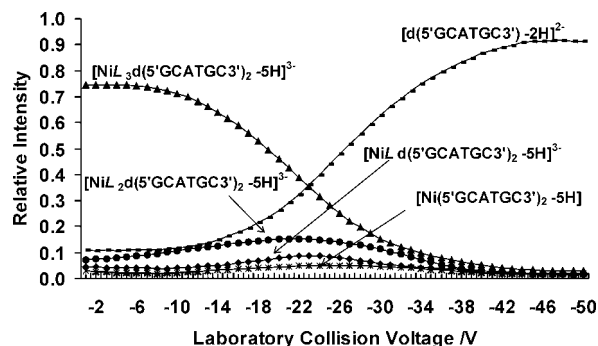
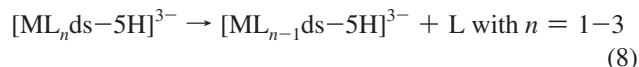


Figure 6. CID profiles for the dissociation of  $[\text{NiL}_3(5'\text{GCATGC}_3')_2 - 5\text{H}]^{3-}$  with  $\text{L} = \text{phen}$ .

complexes to DNA has been under discussion for several years, but there is now a consensus that the binding of ruthenium trisphenanthroline to DNA is external and *not intercalative*.<sup>48</sup>

Here we have investigated the complexation of  $\text{Co}(\text{II})$ ,  $\text{Ni}(\text{II})$ , and  $\text{Cu}(\text{II})$  with 1,10-phenanthroline and double-stranded  $\text{d}(5'\text{GCATGC})$ . No complexation was observed in blank experiments with different electrosprayed solutions of phen and annealed  $\text{d}(5'\text{GCATGC})$ , but mixing in the corresponding metal salts (metal salt:phen:ODN = 5:15:1) resulted in the observation of species with a general formula  $[\text{phen}_n\text{M}_l\text{ds} - (2\text{L} + 3)\text{H}]^{3-}$  where  $n$  is an integer between 1 and  $3\text{L}$ ,  $l = 1, 2$ , and  $3$ ,  $\text{M} = \text{Co}(\text{II})$ ,  $\text{Ni}(\text{II})$ , and  $\text{Cu}(\text{II})$ , and  $\text{ds} = \text{d}(5'\text{GCATGC})_2$ . As many as 3 metal dications and 9 phen ligands were seen to form ternary adducts with the double-stranded ODN. The results of our CID experiments indicate that dissociation proceeds via sequential losses of neutral phen ligands according to eq 8:



A sample CID profile is presented in Figure 6.

The TV values obtained for the ternary adducts containing singly, doubly, and triply ligated complexes of cobalt, nickel, and copper are presented in Table 2 and indicate a slightly enhanced stability of the species containing three ligands (at least for Co and Cu).

The loss of ligand observed with Co, Ni, and Cu as shown in equation 4 is quite different from the strand and charge separation observed in the CID of the trianions of  $\text{d}(5'\text{GCATGC})$  duplex bound to one and two  $[\text{Ru}(\text{phen})_3]^{2+}$  complexes (data not shown). The ruthenium trisphenanthroline in  $[\text{Ru}(\text{phen})_3\text{d}(5'\text{GCATGC})_2 - 5\text{H}]^{3-}$  stayed attached to the strand carrying a single negative charge. So, the observed difference

**TABLE 2: Tangent Voltages (in volts) for the Ternary Adducts of d(5'GCATGC)<sub>2</sub> with Singly, Doubly, and Triply Ligated Phenanthroline Complexes of Co(II), Ni(II), and Cu(II)<sup>a</sup>**

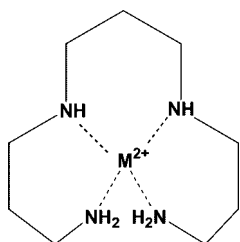
species	[MLds] <sup>3-</sup>	[ML <sub>2</sub> ds] <sup>3-</sup>	[ML <sub>3</sub> ds] <sup>3-</sup>
Co	-26.0 ± 0.3 (0.57)	-25.6 ± 0.3 (0.53)	-36.2 ± 0.4 (0.71)
Ni	-32.2 ± 0.3 (0.73)	-34.6 ± 0.4 (0.72)	-34.1 ± 0.3 (0.69)
Cu	-29.5 ± 0.3 (0.67)	-27.0 ± 0.3 (0.56)	-36.0 ± 0.4 (0.71)

<sup>a</sup> The corresponding apparent center of mass (CM) energies (in electronvolts) are given in parentheses. The apparent center of mass energies were calculated according to  $E_{CM}^R = zTVm_{N_2}(m_{N_2} + m_{ion})^{-1}$  where  $z$  represents the charge of the corresponding parent ion.

**TABLE 3: Tangent Voltages (in Volts) Obtained for the Trianions of Double-Stranded d(5'GCATGC)<sub>2</sub> (ds) with 1, 2, and 3 Tris-Phenanthrolines (L) of Co(II), Ni(II), and Cu(II)<sup>a</sup>**

	Co	Ni	Cu
[ML <sub>3</sub> ds-5H] <sup>3-</sup>	-36.2 ± 0.4 (0.71)	-34.1 ± 0.3 (0.69)	-36.0 ± 0.4 (0.71)
[(ML <sub>3</sub> ) <sub>2</sub> ds-7H] <sup>3-</sup>	-39.0 ± 0.7 (0.68)	-38.1 ± 0.5 (0.67)	-40 ± 1 (0.70)
[(ML <sub>3</sub> ) <sub>3</sub> ds-9H] <sup>3-</sup>	-79 ± 1 (1.23)	-81 ± 1 (1.26)	N/A

<sup>a</sup> The corresponding apparent center of mass (CM) energies (in electronvolts) are given in parentheses. The apparent center of mass energies were calculated according to  $E_{CM}^R = zTVm_{N_2}(m_{N_2} + m_{ion})^{-1}$  where  $z$  represents the charge of the corresponding parent ion.

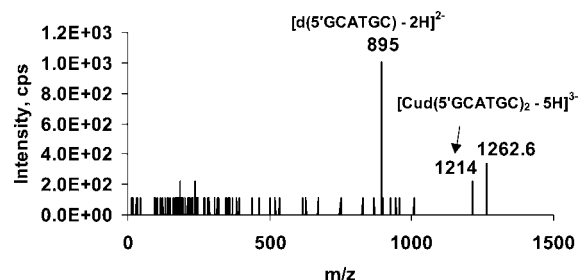
**SCHEME 4**

in the mode of dissociation in the gas phase for the Ru and Co (and Ni and Cu) complexes is consistent with the difference in bonding mode reported for solution.<sup>47,48</sup>

We also specifically compared the relative gas-phase stabilities of the duplex adducts with metallated trisphenanthrolines (Table 3). These complexes are special in that they are completely coordinatively saturated.<sup>49</sup> The ESI spectra of the corresponding M(II)-phen-ODN solutions indicated that no more than three trisphenanthrolines attach to the duplex ODN. This observation is consistent with the nearest neighbor exclusion model<sup>50</sup> which predicts a maximum of 3 for intercalation with a hexameric duplex. Comparison of the relative gas-phase stabilities of the noncovalent adducts of the duplex ODN with 1, 2, and 3 [Mphen<sub>3</sub>]<sup>2+</sup> (Table 3) demonstrates the absence of metal dependence upon the TV values for similar adducts. This is expected if the metal is shielded by the three phen ligands.

Table 3 also shows an unexpected increase in the relative gas-phase stabilities of the adducts with three triply ligated complexes compared to those with two trisphenanthrolines: the TV values increase from ≈0.67 to ≈1.2 eV. This sharp increase in dissociation by the loss of one ligand is puzzling but may be the consequence of enhanced  $\pi$  stacking or the formation of a closer packed structure. Further experiments with longer sequences would be instructive for a better understanding.

**Triethylenetetramine-Cu(II)-d(5'GCATGC)<sub>2</sub> System.** Triethylene tetramine (trien) behaves as a tetradentate ligand in aqueous solution that is capable of forming four coordinative bonds with a metal ion through the lone pairs of its nitrogen atoms, two of which belong to primary amino groups and the other two to secondary ones (Scheme 4).

**Figure 7.** CID spectrum of  $m/z$  1262.6 [Cu-trien-d(5'GCATGC)<sub>2</sub>-5H]<sup>3-</sup> at a laboratory collision voltage of -40 V.

Metal ion-ligand coordination results in the formation of a 10-membered outer chelate ring. Our earlier studies have demonstrated that trien complexes of the first row transition metal dications can be successfully transferred into the gas-phase.<sup>37</sup> Formation of the ternary adduct of the double-strand ODN was observed only in the presence of Cu(II) upon mixing the annealed solution with trien and the corresponding metal salts. This may reflect the much greater thermodynamic stability of [Cu-trien]<sup>2+</sup> complex in aqueous solution,  $\log K = 20$  ( $K$  = stability constant).<sup>51</sup> The CID spectrum of [Cu-trien-d(5'GCATGC)<sub>2</sub>-5H]<sup>3-</sup> indicates a gas-phase dissociation by loss of a neutral trien and further dissociation characteristic of the singly metallated adduct (via separation into two strands) (Figure 7). This dissociation pathway implies that trien ligand chelates copper dication in the gas-phase rather than interacting electrostatically with the polyanionic phosphodiester backbone of the ODN.

**Conclusions**

The results of the research presented here demonstrate that electrospray ionization tandem mass spectrometry provides a versatile tool for the exploration of structural architecture of ternary noncovalently bound adducts of double-stranded DNA and metal complexes. For the systems that were studied, viz. d(5'GCATGC)<sub>2</sub>-ligand-M<sup>2+</sup> (with ligand = BLM, phen, and trien, M = Mn, Fe, Co, Ni, Cu, and Zn), we show that ESI spectra can provide the stoichiometry of the noncovalent complexes formed in solution and the partial characterization of solution equilibria at different solute concentrations, for example, the relative abundance of double-stranded versus single-stranded adducts. The MS/MS experimental results that have been reported provide gas-phase dissociation pathways and relative gas-phase stabilities of ternary adducts of the first row transition metal dications with ligands and DNA. Together, these results offer insight into the binding mode of small antibiotic molecules with double- and single-stranded DNA mediated by metal ions. Generally, there is consistency with the observations of several other research groups who have investigated the MS/MS of DNA-ligand adducts (with no metal present).<sup>12,13,15</sup>

In the literature, we frequently encounter the concept that the ligand binding mode can be deduced from the fragmentation channel in MS/MS. For instance, Wan et al.<sup>19</sup> demonstrated utilizing a quadrupole ion trap that dissociation of the adducts of some minor groove binders with double-stranded DNA proceeds via the loss of a neutral base and covalent breaking of the oligonucleotide, while complexes with intercalators dissociate via noncovalent bond breaking giving the duplex. Similar observations were reported by Rosu et al.<sup>34</sup>

Summarizing the results obtained for the systems studied here, we can suggest a minor groove binding mode for the metallated bleomycins with the double-stranded d(5'GCATGC) (as was



considered a possibility in the solution studies<sup>44</sup>), intercalation for the phen complexes with Cu(II), Co(II), and Ni(II) (as observed in solution for Co(II)<sup>47</sup>), and copper chelation in the gas phase for the trien adduct (no solution data available).

The results presented in this manuscript comprise the first step in developing a new methodology for assaying the intrinsic affinities of a vast array of metalloantibiotics for various types of oligodeoxynucleotide anions: single-stranded versus double-stranded (triplex or quadruplex), hairpins versus duplexes, or complementary versus mismatched.

**Acknowledgment.** Continued financial support from the Natural Sciences and Engineering Research Council of Canada, the National Research Council, and MDS SCIEX is greatly appreciated. As holder of a Canada Research Chair in Physical Chemistry, D.K.B. is thankful for the contributions of the Canada Research Chair Program to this research.

## References and Notes

- (1) Erkkila, K. E.; Odom, D. T.; Barton, J. K. *Chem. Rev.* **1999**, *99*, 2777.
- (2) Hud, N. V.; Polak, M. *Curr. Opin. Struct. Biol.* **2001**, *11*, 293.
- (3) Bianke, G.; Chaurin, V.; Egorov, M.; Lebreton, J.; Constable, E. C.; Housecroft, C. H.; Haider, R. *Bioconjugate Chem.* **2006**, *17*, 1441–1446.
- (4) Ming, L.-J. *Med. Res.* **2003**, *23*, 697, and references therein.
- (5) Giovannelle, C.; Sun, J.-S.; Helene, C. In *Comprehensive Supramolecular Chemistry*; Pergamon: New York, 1996; Vol. 4, p 177.
- (6) Dickerson, R. E. In *Oxford Handbook of Nucleic Acid Structure*; Oxford Science Publications: New York, 1999; p 145.
- (7) Johnson, D. S.; Boger, D. L. In *Comprehensive Supramolecular Chemistry*; Pergamon: New York, 1996; Vol. 4, p 73.
- (8) Yamashita, M.; Fenn, J. B. *J. Phys. Chem.* **1984**, *88*, 4451.
- (9) Fenn, J. B.; Mann, M.; Meng, C. K.; Wong, S. F. *Mass Spectrom. Rev.* **1990**, *9*, 37.
- (10) Gale, D. C.; Smith, R. D. *J. Am. Soc. Mass Spectrom.* **1995**, *6*, 1154.
- (11) Triolo, A.; Arcamone, F. M.; Raffaelli, A.; Salvadori, P. *J. Mass Spectrom.* **1997**, *32*, 1186.
- (12) Kapur, A.; Beck, J. L.; Sheil, M. M. *Rapid Commun. Mass Spectrom.* **1999**, *13*, 2489.
- (13) Gabelica, V.; Rosu, F.; Houssier, C.; De Pauw, E. *Rapid Commun. Mass Spectrom.* **2000**, *14*, 464.
- (14) Gupta, R.; Kapur, A.; Beck, J. L.; Sheil, M. M. *Rapid Commun. Mass Spectrom.* **2001**, *15*, 2472.
- (15) Rosu, F.; Gabelica, V.; Houssier, C.; De Pauw, E. *Nucleic Acids Res.* **2002**, *30*, e82.
- (16) Gabelica, V.; Galic, N.; Rosu, F.; Houssier, C.; De Pauw, E. *J. Mass Spectrom.* **2003**, *38*, 491.
- (17) Gabelica, V.; De Pauw, E. *J. Am. Soc. Mass Spectrom.* **2002**, *13*, 91.
- (18) Gabelica, V.; De Pauw, E.; Rosu, F. *J. Mass Spectrom.* **1999**, *34*, 1328.
- (19) Wan, K. X.; Gross, M. L.; Shibue, T. *J. Am. Soc. Mass Spectrom.* **2000**, *11*, 450.
- (20) Reyzer, M. L.; Brodbelt, J. S.; Kerwin, S. M.; Kumar, D. *Nucleic Acids Res.* **2001**, *29*, e103.
- (21) David, W.; Kerwin, S. M.; Kern, J.; Brodbelt, J. M. *Anal. Chem.* **2000**, *74*, 2029.
- (22) Oehlers, L.; Mazzitelli, C.; Rodriguez, M.; Brodbelt, J. S.; Kerwin, S. *J. Am. Soc. Mass Spectrom.* **2004**, *15*, 1593.
- (23) Keller, K. M.; Breeden, M. M.; Zhang, J.; Ellington, A. D.; Brodbelt, J. S. *J. Mass Spectrom.* **2005**, *40*, 1327.
- (24) Keller, K. M.; Zhang, J.; Oehlers, L.; Brodbelt, J. S. *J. Mass Spectrom.* **2005**, *40*, 1362.
- (25) Mazzitelli, C. L.; Kern, J. T.; Rodriguez, M.; Brodbelt, J. S.; Kerwin, S. *J. Am. Soc. Mass Spectrom.* **2006**, *17*, 593.
- (26) Shi, X.; Takamizawa, A.; Nishimura, Y.; Hiraoka, K.; Akashi, S. *J. Mass Spectrom.* **2006**, *41*, 1086.
- (27) Wu, J.; McLuckey, S. A. *Int. J. Mass Spectrom.* **2004**, *237*, 197.
- (28) Ruan, C.; Hai, H.; Rodgers, M. T. *J. Am. Soc. Mass Spectrom.* **2008**, *19*, 305.
- (29) Zhibo, Y.; Rodgers, M. T. *J. Phys. Chem. A* **2006**, *110*, 1455.
- (30) Anichina, J.; Feil, S.; Uggerud, E. Bohme, D. K. *J. Am. Soc. Mass Spectrom.* **2008**, *19*, 987.
- (31) Beck, J. L.; Colgrave, M. L.; Ralph, S. F.; Sheil, M. M. *Mass Spectrom. Rev.* **2001**, *20*, 61.
- (32) Keller, K. M.; Brodbelt, J. S. *J. Am. Soc. Mass Spectrom.* **2005**, *16*, 28.
- (33) Baker, E. S.; Bernstein, S. L.; Gabelica, V.; De Pauw, E.; Bowers, M. T. *Int. J. Mass Spectrom.* **2006**, *253*, 225.
- (34) Rosu, F.; Pirotte, S.; De Pauw, E.; Gabelica, V. *Int. J. Mass Spectrom.* **2006**, *253*, 156.
- (35) Rosu, F.; Nguen, C. - H.; De Pauw, E.; Gabelica, V. *J. Am. Soc. Mass Spectrom.* **2007**, *18*, 1052.
- (36) Zimmer, C.; Wahnert, U. *Prog. Biophys. Mol. Biol.* **1986**, *47*, 31.
- (37) Anichina, J.; Bohme, D. K. *Int. J. Mass Spectrom.* **2007**, *267*, 256.
- (38) Anichina, J.; Zhao, X.; Bohme, D. K. *J. Phys. Chem. A* **2006**, *110*, 10763.
- (39) Cooper, G. M.; Hausman, R. E. In *The Cell: A Molecular Approach*, 4 ed.; Sinauer Associates, Inc; ASM Press: Washington, DC, 2004.
- (40) Pan, S.; Sun, X.; Lee, J. K. *J. Am. Soc. Mass Spectrom.* **2006**, *17*, 1383.
- (41) Aoki, K. In *Comprehensive Supramolecular Chemistry*; Pergamon: New York, 1996; Vol. 5, p 249.
- (42) Wang, Y.; Taylor, J.-S.; Gross, M. L. *J. Am. Soc. Mass Spectrom.* **2001**, *12*, 550.
- (43) Chen, J.; Stubbe, J. *Curr. Opin. Chem. Biol.* **2004**, *8*, 175.
- (44) Hecht, S. M. *J. Nat. Prod.* **2000**, *63*, 158.
- (45) Kopka, M. L.; Larsen, T. A. In *Nucleic Acid Targeted Drug Design*; Dekker: New York, 1992; p 303.
- (46) Barton, J. K.; Dupureur, C. M. In *Comprehensive Supramolecular Chemistry*; Pergamon: New York, 1996; Vol. 5, p 295.
- (47) Niu, S.; Li, F.; Zhang, S.; Wang, L.; Li, X.; Wang, S. *Sensors* **2006**, *6*, 1234.
- (48) Coggan, D. Z. M.; Haworth, I. S.; Bates, P. J.; Robinson, A.; Rodger, A. *Inorg. Chem.* **1999**, *38*, 4486.
- (49) Arif, M.; Chohan, Z. H.; Burkhari, J. H.; Anjum, S.; Tarq, R. H. *Rev. Inorg. Chem.* **2006**, *26*, 379.
- (50) Schellman, J. A.; Reese, H. R. *Biopolymers* **1996**, *39*, 161.
- (51) NIST. *Critical Stability Constants of Metal Complexes*; 2004; version 8.

JP807034V